

## Study of Tunnel Magneto-Resistance in Junctionless Magnetoresistive Device Based On Passivated Zigzag Gallium Nitride Nano-Ribbon

Akanksha Thakur\*

University of Petroleum and Energy Studies, Dehradun, Uttarakhand, India

\*Corresponding author: Akanksha T, University of Petroleum and Energy Studies, Dehradun, Uttarakhand, India, Tel: +91-9165427559; E-mail: akankshathakur1002@gmail.com

**Copyright:** © 2022 Akanksha T. This is an open-access article distributed under the terms of the Creative Commons Attribution License, which permits unrestricted use, distribution, and reproduction in any medium, provided the original author and source are credited.

**Received date:** January 03, 2022; **Accepted date:** January 20, 2022; **Published date:** January 27, 2022

### Abstract

For investigating the magneto-resistive property of junctionless magnetoresistive device (JMD), first principle density functional theory calculations along with non-equilibrium Green's function (NEGF) method is used. In this work the magnetoresistance of edge passivated zigzag gallium nitride nano-ribbons (ZGaNNR) have been computed. Though the gallium nitride is non-magnetic material but for small length till 1.7 nm it shows magnetism. The result of this calculation indicates that the electrical property of ZGaNNR can be changed by passivating the edges of nano-ribbons with hydrogen (H) and fluorine (F) atoms. When passivating both edges of nanoribbons with H and F atoms it gives a semiconducting ZGaNNR. When passivating the edge consisting gallium atoms with H and F atoms it results in a half metallic ZGaNNR. A JMD can be constructed by passivating particular edges of nano-ribbon, the electrodes should be half metallic and the central scattering region should be semiconducting. The JMD with H passivation provides higher magneto-resistance (MR) and much better spin filtering efficiency in comparison to JMD with F passivation. The major application of these kind of devices is in making Magneto-Resistive Random Access Memories (MRAMs).

### Introduction

Spintronics, a continuously evolving field of research in physics as well as engineering that has target to utilize the electron spin in solid state materials and many more fields [1,2]. The devices made with the use of Spintronics, they utilize the property of electron's spin along with it's charge to carry information so that they can offer novel nano electronic devices [3]. Spin based devices have massive applications in various electronic and other fields such as programmable logic elements (PLE), Magnetoresistive Random Access Memory and magnetic sensors. The property called half metallicity is very useful for creating any spintronic device [4-6]. The half metallicity property has been applied in a huge scale of nanoelectronics along with different materials like double layer perovskites and alloys.[7- 10]. The

discovery of Giant Magnetoresistance and Tunnel Magnetoresistance led to the progress of spintronics. The Magnetic Tunnel Junction (MTJ) is one such device of spintronics that made revolutionary changes in the field of research [11,12]. MTJ consists of two layers (electrodes) of magnetic metal or semimetals, separated by a very thin dielectric layer ranges from few angstroms to a few nanometers. The insulating or dielectric layer is also called as tunnel barrier because electrons can tunnel through the thin layer of dielectric material [16-18]. The tunnelling current of MTJ depends on two configurations of intrinsic spin one is parallel configuration (PC) in which both spin orientations of electrodes are same and the other one is anti-parallel configuration (APC) in which both spin orientations of electrodes are different [19]. Usually MTJs provide low resistance in PC and high resistance in APC, this property of MTJ gives rise to a very important Phenomenon called tunnel magneto-resistance (TMR). The most famous application of MTJ is MRAM. MRAM combines the best properties of SRAM, DRAM and flash memories. For tunnel barriers usually magnesium oxide MgO and aluminium oxide Al<sub>2</sub>O<sub>3</sub> is used which is sandwiched between the two layers of electrodes, but their performance is restricted to some extent because of the defects in oxides. Now a days graphene and alike other 2D materials are used as a tunnel barrier because they are only one atom thick materials so an electron can easily tunnel from one electrode to another electrode [20,21]. Here in this paper polycrystalline Gallium Nitride (GaN) is used as barrier and as well as electrodes. One can achieve better spin filtration and high magnetoresistance by using same material for tunnel barrier and electrodes, which is proposed as JMD [22,23]. JMD can be the best alternative of MTJ because it is junctionless and it consumes less space and gives better performance. Zigzag gallium nitride GaN nanoribbon (ZGaNNR) works as a semiconductor when it is passivated with fluorine and hydrogen on the both edges of unit cell as given in Figure 1(a,c) and is used as tunnel barrier or central region of JMD in Figure 1(b,d) Zigzag GaN nanoribbon can work as Half Metallic Ferromagnet (HMF) when it is passivated on gallium edge by fluorine and hydrogen and is used as electrodes of JMD. The conductivity modulation is possible on passivating the nano-ribbons with hydrogen and fluorine which can be confirm with [24]. Spin transport properties in JMD with hydrogen- and fluorine-passivation is calculated in this paper.

### Computational Methods and details

For analysing of spin transport property and material property in spintronic devices like JMD, simulation package of Synopsis Atomistix Toolkit Virtual NanoLab software is used. By using Density Functional Theory (DFT) along with NEGF method the transport analysis of materials, atoms, molecules and nano- systems becomes very convenient [25,26]. The JMD consists of passivated ZGaNNR is simulated with the help of ATK VNL software. In Fig.3 JMD passivated with hydrogen is shown, whereas in Figure 4, JMD passivated with fluorine is shown. In both the structures the electrodes are HMF and the tunnel barrier region is semiconducting. Both the structures are simulated for parallel as well as anti-parallel configurations. After the geometry optimization or relaxation the bond length of gallium nitride structure is 1.8 Å. Tunnel barrier is constructed by passivation of hydrogen on both the edges of the ZGaNNR (termed as ZGaNNR-2H) in Figure 3 and passivation with fluorine (termed as ZGaNNR-2F) in Figure 4. Electrodes are constructed by passivating the Gallium edge of zigzag GaN

nanoribbon with fluorine (termed as ZGaNRR-FGa) shown in Figure 3 and by passivating the Gallium edge of zigzag GaN nanoribbon with hydrogen (termed as ZGaNRR-HGa) shown in Figure 4. The building block for each type of ZGaNRRs was sampled by using the k-point sampling set of  $1 \times 1 \times 300$  for calculating bandstructure and density of states (DOS) with periodic boundary conditions along z-axis. For exchange correlation Linear Combination of Atomic Orbitals (LCAO) basis set along with Local Spin Density Approximation (LSDA) is used. LDA is used instead of generalized gradient approximation (GGA) because the GGA method underrates surface-impurity interactions [27,28]. The mesh cut-off energy of 100 Rydberg. Double-Zeta Plus (DGP) polarized basis set is used for Gallium, Hydrogen, Nitrogen and Fluorine atoms. K point sampling  $1 \times 1 \times 300$  is used for all the calculations. After relaxation all the atoms of both the structures comes under the force less than 0.05 eV/Å. For PC both the electrodes were set to spin up state and for APC one electrode is set to spin up state and one electrode is set to spin down state [29].

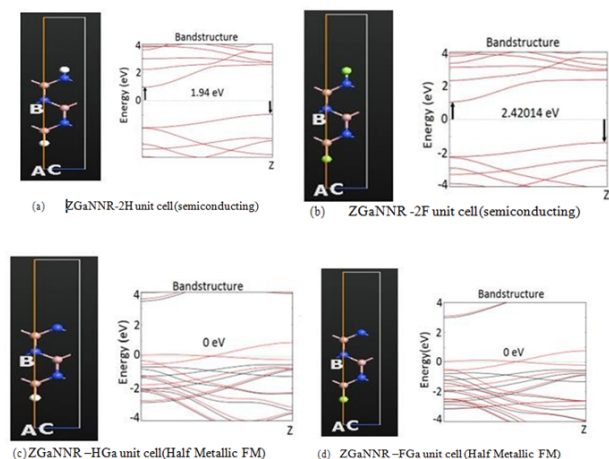


**Figure 1:** Unit cell of ZGaNRR with H (a,c) and F (b,d) passivation. In band structures red and black line corresponds to down and up spin states.

## Results and Discussion

ZGaNRR shows semiconducting property on passivating with hydrogen and fluorine on both upper and lower side of nanoribbon the bandgaps are 1.94 eV and 2.42 eV respectively. Its density of states (DOS) also shows their semiconducting properties in Figure 2. ZGaNRR shows half metallic property on passivating with hydrogen and fluorine on the edge of Gallium atoms only it can be seen by bandstructures and DOS in Figure 2.

The property of half metallicity of ZGaNRRs can be observed by the band structure, the energy bandgap is zero (0) for the spin down state, however energy gap is present in up spin state. From DOS also the property of half metallicity can be observed the DOS is different for both spin up (black line) and down (red line) state.

For the down spin nanoribbon acts as conductor and for the up spin nanoribbon acts as insulator. The H passivated JMD is shown in Figure 3 Half Metallic Ferromagnetic electrodes sandwiched with

semiconducting region in JMD. The F passivated JMD is shown in Figure 4. The width and length of central semiconducting regions are 6.12 Å and 23.64 Å respectively for both the structures. In Figure 5 (a,b) the I-V characteristics of hydrogen-passivated JMD for both PC and APC are shown. Current is found more in PC than in APC.

The current is same in up and down state in PC at 0 V, but as the voltage increases the current of spin up state is also increases till 200 nA at bias voltage 0.25 V and at the same time the current of spin down state remains negligible. In APC the current is small and this graph also the current of spin up state is greater than the current of spin down state. In Figure 5 (c,d) The I-V characteristics of fluorine passivated JMD for both PC and APC are shown. Similar to H passivated JMD the value of current in PC is greater than in APC.

In H passivated device also the current of spin up state is same as current in spin down state at 0V, but as the voltage increases the spin up current also increases till 800 nA at bias Voltage 0.25 V and at the same time the spin down current remains negligible.

Like the H passivated JMD device in F passivated device the current in spin up state is greater than the current in spin down state. F-passivated JMD shows more current than in H-passivated JMD in PC and in APC current is similar in both the devices. A very good spin filtering shown in Figure 5 for spin up electron. Spin down current should be zero in APC for high spin filtration and high magnetoresistance.

The transmission spectrums of spin up and down state in PC and APC are shown in Fig. 6. In this study one can observe that only one type of spin electrons can contribute to current in such case spin-up electron. Due to this property great spin filtration is observed by HMF electrodes. Both fluorine and hydrogen passivated JMD structures provides the spin-up current in PC which can be verified by the transmission spectrum (Figure 6a).

The electronic states near Fermi level indicates that they are contributing to conduction of current. For fluorine as well as hydrogen passivated JMD spin down electrons can't contribute to conduction of current in PC (Figure 6b).

The peaks of transmission energy are higher in hydrogen passivated device than in fluorine passivated device which shows higher current in H-passivated device in PC (Figure 5), current in APC is comparatively small (see Figure 5) which can be verified by transmission peaks as they are so far from Fermi energy level (Figure 6).

The efficiency of spin is computed by the definition  $\eta = (I_{\uparrow} - I_{\downarrow}) / (I_{\uparrow} + I_{\downarrow})$ . The efficiency is better in Hydrogen passivated JMD than in fluorine passivated JMD in PC and the efficiency of H passivated JMD is almost similar to F passivated JMD in APC configuration (Figure 7).

For the computation of Magneto Resistance (MR) in Figure 8 the I-V curves (Figure 5) are used at different bias voltages. Magneto resistance is computed by the definition:  $MR = (IPC - IAPC) / IPC$ . Here, IPC and IAPC denote the total current in PC and APC respectively. For the calculation of MR at zero bias voltage the property called equilibrium conductance can be used because the current for both spin up and down is zero at zero bias voltage. [29-32].

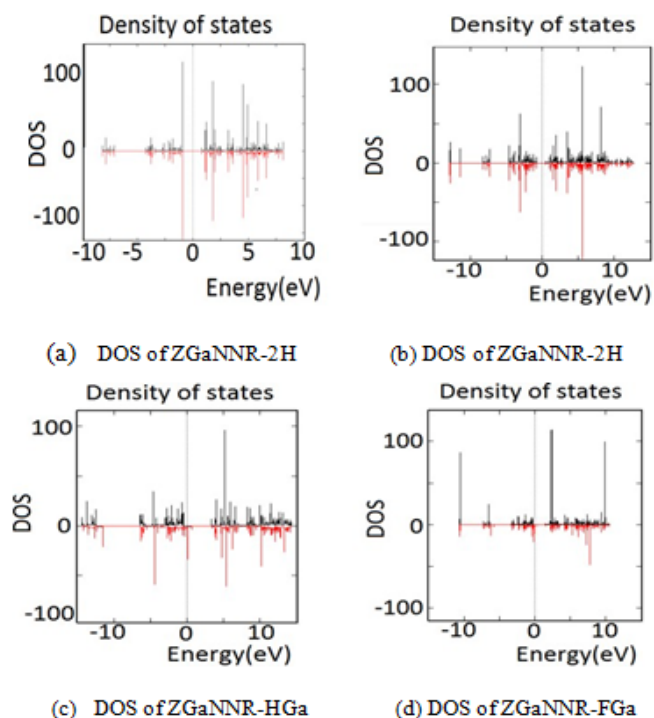


**Figure 2:** Density Of States of ZGaNNR with both the sides passivated (a,b and only Gallium side passivated (c,d) Fermi level is at 0 eV.

By analysing transmission energy peaks near Fermi level one can predict the change in current with particular bias voltages.

In APC current is less because transmission peaks are zero near Fermi level however in PC current is more because there are visible transmission peaks near Fermi level.

In various research works [33-35] which are done previously, the similar results can be seen and justified. At different bias voltage we can see different current.

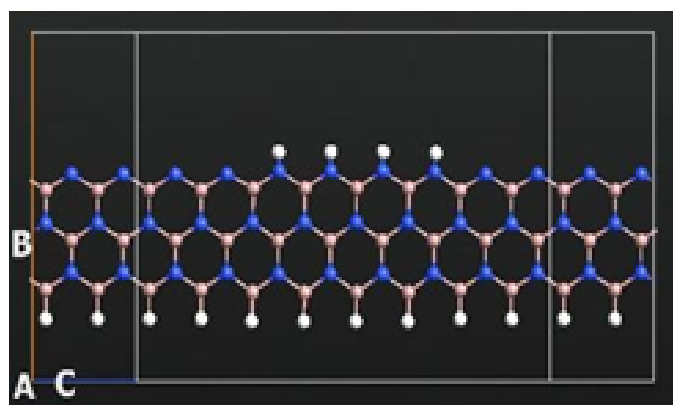


**Figure 3:** H-passivated JMD structure. The tunnel barrier region is semiconducting and the electrodes are half metallic ferromagnetic. The length of semiconducting region is 23.64 Å and width of ZGaNNR is 6.12 Å.

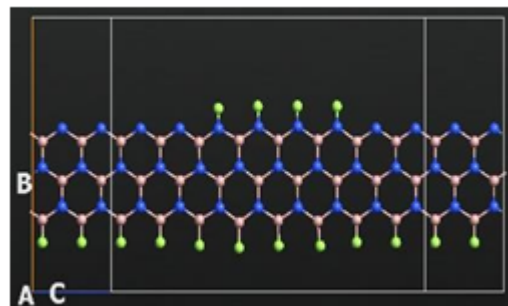


**Figure 4:** F-passivated JMD structure. The tunnel barrier region is semiconducting, and the electrodes are half metallic ferromagnetic. The length of central region is 23.64 Å and width of ZGaNNR is 6.12 Å.

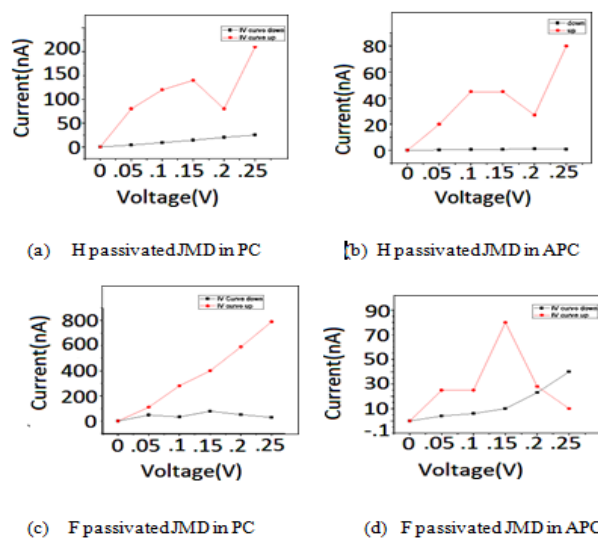


**Figure 5:** I-V characteristics of JMD structures.

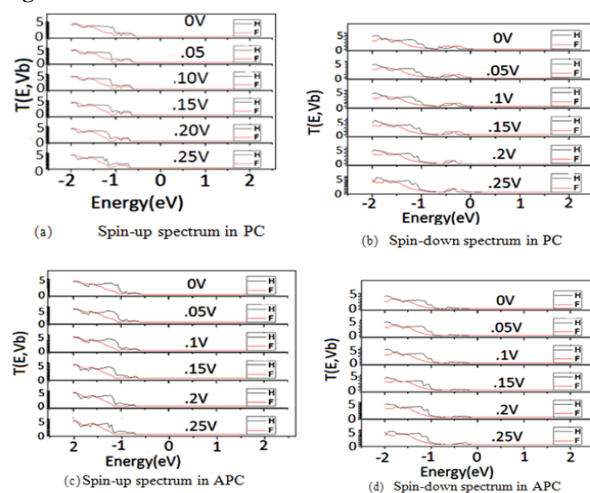


**Figure 6:** Transmission energy spectrum  $[T(E,Vb)]$  in spin-up and spin-down state in PC and APC. Red line in the graph shows F- JMD and black line in the graph shows the spectrum for H- JMD. Fermi level is at 0 eV.

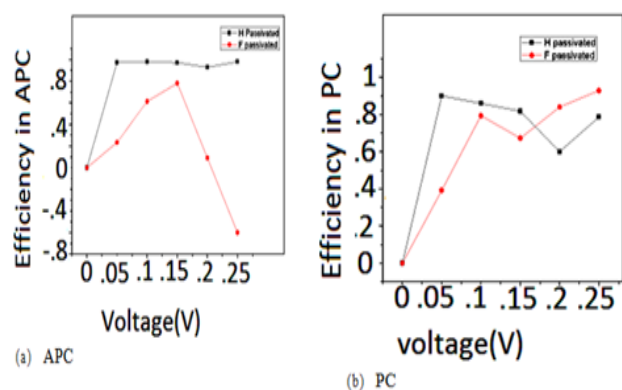


**Figure 7:** Efficiency of the JMD structure in Parallel and Anti-parallel configurations.

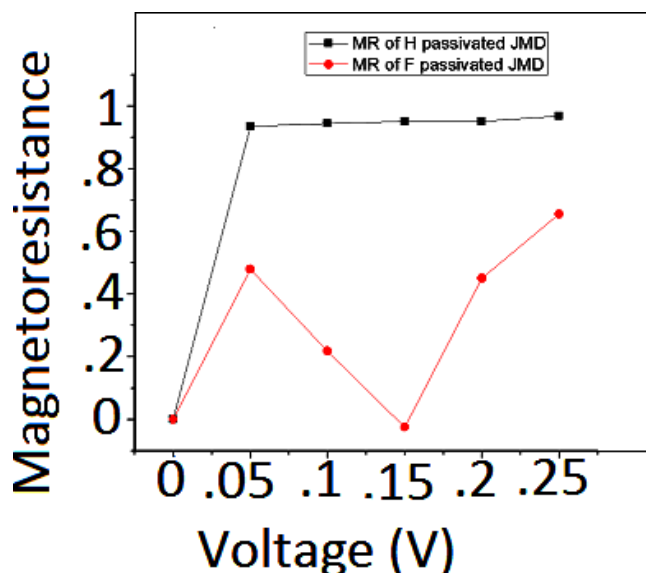


**Figure 8:** Magnetoresistance of JMD structure.

## Conclusion

On the basis of above calculations, it may be concluded that the analysis of magnetoresistive property of ZGaNNR has successfully been performed by using first principle density functional (DFT) approach. 2D JMD can be constructed by using two properties semiconducting and HMF acquired by adjusting the conductivity of ZGaNNR. With the help of H and F atoms passivated nanoribbon one can convert a ZGaNNR into semiconducting and HMF. When ZGaNNR passivated with H and F on upper and lower sides it becomes semiconducting and when ZGaNNR passivated with hydrogen and fluorine on gallium side it becomes half metallic ferromagnetic (HMF). Hydrogen passivated device gives higher MR and better spin filtration efficiency when compared with fluorine passivated device. The device is junctionless so it is less complex to fabricate.

## References

1. Wang B, Zhu Y, Ren W, Wang J, Guo H (2007) Spin- dependent transport in Fe-doped carbon nanotubes. *Phys Rev B* 75: 235415.

2. Yao KL, Min Y, Liu ZL, Cheng HG, Zhu SC, et al. (2008) First-principles study of transport of Vdoped boronnitride nanotube. *Phys Lett A* 372: 5609-5613.

3. Lai L, Lu J (2011) Half metallicity in BC<sub>2</sub>N nanoribbons: stability, electronic structures, and magnetism. *Nanoscale* 3: 2583-2588.

4. Lin X, Ni J (2011) Half-metallicity in graphene nanoribbons with topological line defects. *Phys Rev B* 84: 075461.

5. Liu Y, Wu X, Zhao Y, Zeng XC, Yang J (2011) Half-metallicity in hybrid graphene/boron nitride nanoribbon with dihydrogenated edges. *J Phys Chem C* 115: 9442-9450.

6. León C, Latgé A (2013) Half-metallicity study of graphene nanoribbon bilayers under external fields. *Phys Rev B* 88: 245446.

7. Lin Y, Connell JW (2012) Advances in 2D boron nitride nanostructures: nanosheets, nanoribbons, nanomeses, and hybrids with graphene. *Nanoscale* 4: 6908-6939.

8. Li X, Wu X, Yang J (2014) Room-Temperature Half-Metallicity in La(Mn,Zn)AsO Alloy via Element Substitutions. *J Am Chem Soc* 136: 5664-5669.

9. Groot RA, Mueller FM, Engen PG, Buschow KHJ (1983) New class of materials: half- metallic ferromagnets. *Phys Rev Lett* 50: 2024.

10. Alijani V, Winterlik J, Echer GH, Naghavi SS, Felser C (2001) Quaternary half-metallic Heusler ferromagnets for spintronics applications. *Phys Rev B* 63: 184428.

11. Kobayashi KI, Kimura T, Sawada H, Terakura K, Tokura Y (1998) Room-temperature magnetoresistance in an oxide material with an ordered double-perovskite structure. *Nature* 395: 677-680.

12. Kobayashi KI, Kimura T, Tomioka Y, Sawada H, Terakura K, et al. (1999) Intergrain tunneling magnetoresistance in polycrystals of the ordered double perovskite Sr<sub>2</sub>FeReO<sub>6</sub>. *Phys Rev B* 59: 11159.

13. Galanakis I, Mavropoulos P (2003) Zinc-blende compounds of transition elements with N, P, As, Sb, S, Se, and Te as half-metallic systems. *Phys Rev B* 67: 104417.

14. Xie WH, Xu YQ, Liu BG, Pettifor DG (2003) Half-metallic ferromagnetism and structural stability of zincblende phases of the transition-metal chalcogenides. *Phys Rev Lett* 91: 037204.

15. Liu BG (2005) Half-metallic ferromagnetism and stability of transition metal pnictides and chalcogenides, in Half- Metallic Alloys. 676.

16. Sato M, Kikuchi H, Kobayashi K (1999) Effects of interface oxidization in ferromagnetic tunnel junctions. *IEEE Trans Magn* 35: 2946-2948.

17. Ikeda S, Hayakawa J, Lee YM, Matsukura F, Ohno Y, et al. (2007) Magnetic tunnel junctions for spintronic memories and beyond. *IEEE Trans Electron Devices* 54: 991-1002.

18. Maekawa S, Gafvert U (1982) Electron tunneling between ferromagnetic films. *IEEE Trans Magn* 18: 707-708.

19. Nowak J, Rauluszkiwicz J (1992) Spin dependent electron tunnelling between ferromagnetic films. *J Magn Magn Mater* 109: 79-90.

20. Cobas E, Friedman AL, Erve OMJ, Robinson OMJ, Jonker BT (2013) Graphene based magnetic tunnel junctions. *IEEE Trans Magn* 49: 4343-4346.

21. Li W, Xue L, Abruna HD, Ralph DC (2014) Magnetic tunnel junctions with single-layer-graphene tunnel barriers. *Phys Rev B* 89: 184418.
22. Lee SM, Lee YH, Hwang YG (1999) Stability and electronic structure of GaN nanotubes from density functional calculations. *Phys Rev B* 60: 7788-7791.
23. Piquemal-Banci M, Galceran R, Martin MB, Godel F, Anane A, et al. (2017) 2D- MTJs: introducing 2D materials in magnetic tunnel junctions. *J Phys D Appl Phys* 50: 203002.
24. Wu M, Wu X, Pei Y, Zeng XC (2011) Inorganic nanoribbons with unpassivated zigzag edges: Half metallicity and edge reconstruction. *Nano Res* 4: 233-239.
25. [www.quantumwise.com](http://www.quantumwise.com).
26. Perdew JP, Zunger A (1981) Self-interaction correction to density-functional approximations for many electron systems. *Phys Rev B* 23: 5048.
27. Zhao J, Buldum A, Han J, Lu JP (2002) Gas molecule adsorption in carbon nanotubes and nanotube bundles. *Nanotechnology* 13: 195.
28. Rai HM, Saxena SK, Mishra V, Kumar R, Sagdeo PR, et al. (2015) Half metallicity in armchair boron nitride nanoribbons: A first-principles study. *Solid State Commun* 212: 19-24.
29. Choudhary S, Mishra P, Goyal R (2016) First-principles study of spin transport in BN doped CrO<sub>2</sub>-graphene-CrO<sub>2</sub> magnetic tunnel junction. *Phys Lett A* 380: 1098-1101.
30. Meena S, Choudhary S (2017) Tuning the tunneling magnetoresistance by using fluorinated graphene in graphene based magnetic junctions. *AIP Adv* 7: 125008.
31. Kumar A, Choudhary S (2018) Enhanced magnetoresistance in in-plane monolayer MoS<sub>2</sub> with CrO<sub>2</sub> electrodes. *J Supercond Nov Magn* 3: 1-6.
32. Chakraverty M, Kittur HM, Arun Kumar P (2013) First principle simulations of various magnetic tunnel junctions for applications in magnetoresistive random access memories. *IEEE Trans Nanotechnology* 12: 971-977
33. Choudhary S, Qureshi S (2011) Theoretical study on transport properties of a BN co-doped SiC nanotube. *Phys Lett A* 375: 3382-3385.
34. Choudhary S, Qureshi S (2011) Theoretical study on the effect of vacancy defect reconstruction on electron transport in Si-C nanotubes. *Mod Phys Lett B* 25: 2159-2170.
35. Choudhary S, Qureshi S (2012) Effect of moisture on electron transport in SiC nanotubes: an ab initio study. *Phys Lett A* 376: 3359-3362.